ISSN 2070-2051, Protection of Metals and Physical Chemistry of Surfaces, 2020, Vol. 56, No. 4, pp. 766–771. © Pleiades Publishing, Ltd., 2020.

NANOSCALE AND NANOSTRUCTURED MATERIALS AND COATINGS

Modified Mechanical Coating Technique for the Preparation of Nanohydroxyapatite Coated Ti–6Al–4V Dental Implants

Hossein Ahmadzadeh[a], Taghi Isfahani[a, *, **], and Anoosheh Zargar Kharazi[b]

[a] *Metallurgy & Materials Engineering Department, Golpayegan University of Technology, Golpayegan, P. O. Box: 87717-65651 Iran*

[b] *Biomaterials Nanotechnology and Tissue Engineering Faculty, School of Advanced Technologies in Medicine, Isfahan University of Medical Sciences, Isfahan, 8174673461 Iran*

**e-mail: t.isfahani@yahoo.com*

***e-mail: tdi1359@iust.ac.ir*

Received July 30, 2018; revised January 12, 2020; accepted March 15, 2020

Abstract—To improve the mechanical and biological properties and also to increase the lifetime and performance of Ti–6Al–4V dental implants they were coated by hydroxyapatite nanoparticles using a modified mechanical coating technique. A novel milling vial was developed to simultaneously coat hydroxyapatite nanoparticles on the Ti–6Al–4V substrates. The modified dimensions of the milling vial and optimized milling operation parameters were presented. The coating operation was applied for 4 hours with a ball to powder weight ratio of 30 : 1. Furthermore the bioactivity of the coatings was studied by placing the coating in a simulated body fluid for 14 days. SEM and FTIR analysis indicated the bone bonding ability of the coating by its capability of forming hydroxyapatite on the surface of the coating. The coating operation resulted in the formation of a uniform nanoparticle containing coating and significantly decreased the cost and complexity of the nanohydroxyapatite coating process on Ti–6Al–4V substrates.

Keywords: mechanical coating, milling vial, dental implants, bioactivity, hydroxyapatite

DOI: 10.1134/S2070205120040036

1. INTRODUCTION

There is a vital need for biomaterials to replace bones, teeth and organs and their functions. The interactions between natural tissues and biomaterials have become of great concern. For this reason interests for the design and fabrication of new biocompatible and bioactive materials have increased. For this reason researchers are looking for new biomaterials with advanced mechanical and biological properties or to develop new technologies for the enhancement of those properties in usual biomaterials [1].

Metallic implants especially titanium and its alloys have been widely used in the medical and dental field because of their excellent biocompatibility and good mechanical properties [2–5], light weight as well as their resistivity against corrosion [6, 7]. Some of their applications are in orthopedic surgeries and dental implants these implants usually provide the needed mechanical properties while having weak bioactivity properties. In other words their long period to obtain good fixation between that material, teeth and bone [8] is a serious disadvantage of them. However to shorten the bone fixation term, various surface modification techniques and implant driven treatment considerations have been attempted [9–11]. A number of studies have attempted to use various bioactive coatings on to the surface of titanium implants in order to improve the implant osseo integration [12–14]. Therefore to overcome these problems, bioceramic coatings are used on the surface of the implants in order to improve the connection between tissue and implant, decrease the corrosion and release of metal ions in the surrounding tissues of the implants and finally to improve the biocompatibility. As mentioned by many researchers between all the reported bioceramics hydroxyapatite is the best candidate for coating metallic implants [15–17].

Hydroxyapatite with $C_{10}(PO_4)_6(OH)_2$ composition is a bioactive material with biocompatibility and osseo integration potential and is structurally similar to apatite which is the mineral component of bone [18]. For this reason it is used to fill injured bones, make bone scaffolds and metal implant coatings [19, 20]. Although hydroxyapatite is a good candidate for bone grafting, but its mechanical characteristics like low strength and high brittleness limits its use in orthopedic applications, especially for implants under load. This leads to the inconsistency of implants in the physiological environment of the body [21, 22]. Also, pure hydroxyapatite suffers a relatively high dissolu-

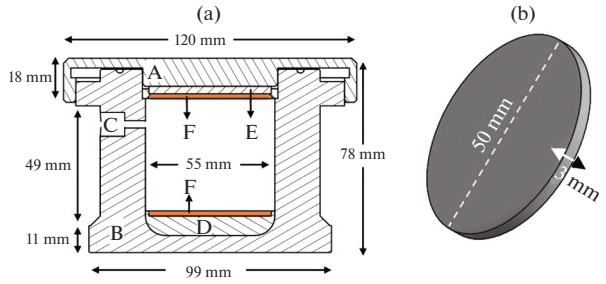

Fig. 1. (a) The design of the new and optimized milling vial (b) dimensions of the used substrate (part F in the Fig. 1a).

tion rate in simulated body fluid that affects its long term stability [23]. To overcome this limit, hydroxyapatite composites or hydroxyapatite coatings on bioactive ceramics and metals can be used which totally enhance the mechanical characteristics along with keeping the bioactivity and biocompability of the hydroxyapatite and can be used to be involved in the repair of bone defects, bone augmentation, as well as coating on the metallic implants of human body [24–26]. However in some cases a desirable flexibility still may not be obtained which has to be overcome [27].

Common coating methods include sol-gel method, physical and chemical vapor deposition and hot dip coating. Besides the advantages of these methods, they also have some limitations such as difficulties in the coating mechanism and being costly and time-consuming [28–30]. Therefore one of the main purposes of this study is to design a milling vial able to simultaneously and uniformly coat on the substrates by mechanical coating technique to reduce the time and cost of the procedure. The other aim of this research is to use the designed milling vial and coat hydroxyapatite particles on Ti–6Al–4V substrates using optimized milling conditions to form uniform bioactive nanohydroxyapatite coatings. Therefore a successful physical coating with hydroxyapatite on Ti–6Al–4V alloys can obtain good mechanical properties and excellent bone fixation and combine the favorable mechanical properties of titanium alloy and the excellent biocompatibility and bioactivity of hydroxyapatite.

2. MATERIALS AND METHOD

In this section the optimized design and dimensions of the milling vial used for coating hydroxyapatite nanoparticles by mechanical coating is presented. Then the resulting coating is analyzed by scanning electron microscope (SEM), X-ray diffraction (XRD) and Fourier transform infrared (FTIR) to determine the particle size and shape, the structure and crystallite size. The bioactivity of the coating is investigated using FTIR analysis after insertion into the simulated body fluid for 14 days.

2.1. Design and Parameters of the Milling Vial

2.1.1. Design and the material of the milling vial. To make the milling vial, tool steel 1.2080 was heat treated after the machining process to increase its hardness. Figure 1 schematically shows a complete view of the new and optimized milling vial which was obtained after optimizing the dimensions of the vial.

Section A in Fig. 1a shows the location of the cap of the milling vial. Section B shows the main body of the vial while section C shows the location of the valves provided to control the atmosphere and purge argon gas into the vial to prevent oxidation during the process. Sections D and E show the locations where the two substrates are placed for mechanical coating technique one at the top and another at the bottom. Sections F are the substrates to be coated and are marked in red color. Based on Fig. 1b the diameter and thickness of the disk shaped substrates are defined. The maximum diameter is 50 mm where the maximum thickness can be 5 mm. After the coating operation is completed, both sections D and E are removed out of the vial and the two coated substrates are ready to be removed. Therefore the removal of the coated substrates from the vial is done safely and easily without leaving any pollution, deterioration or possible damage. Even when the coating operation is not needed and only a simple milling operation is to be used, sections D and E can be removed and the interior part of the vial is free to be used in the milling process. Depending on the thickness of the chosen substrate the thickness of section F can be changed between 1 to 5 millimeters. This freedom in choosing substrate thickness obviously is one of the advantages of the designed vial. As shown in figure 1a circular deep groove is provided to hold and fix the upper substrate where the vial cap is in contact with. By placing an O-ring with the proper thickness the gap between the door and the body is filled. In this way the probability of having pollution and argon leakage from the outside will be completely prevented. Therefore there is enough free space inside the vial for the balls so that different balls with different diameters can easily move while only half of the space is filled. Then the vial is placed into the planetary milling machine and the optimization of the coating condition is obtained having continuous moving of the balls and the impacting of the upper and lower substrate so that the powder completely covers the substrates.

2.2. Coating Conditions

The coating obtained inside the designed vial was done using 4 grams of synthesized hydroxyapatite powder (as described below) along with 11 stainless steel balls of 10 millimeter diameter, 33 balls with

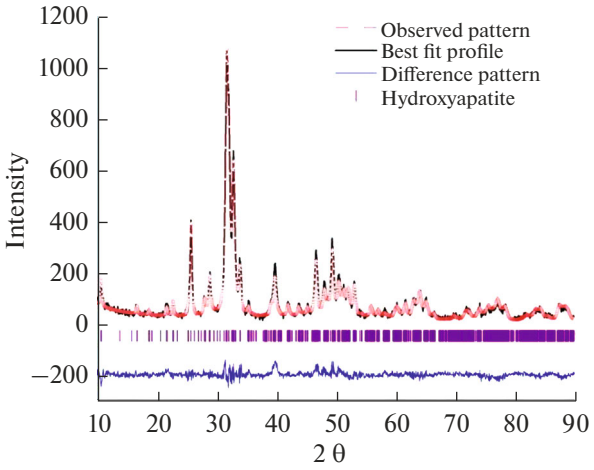

Fig. 2. X-ray diffraction pattern and Rietveld analysis of the hydroxyapatite nanopowder used for the coating process.

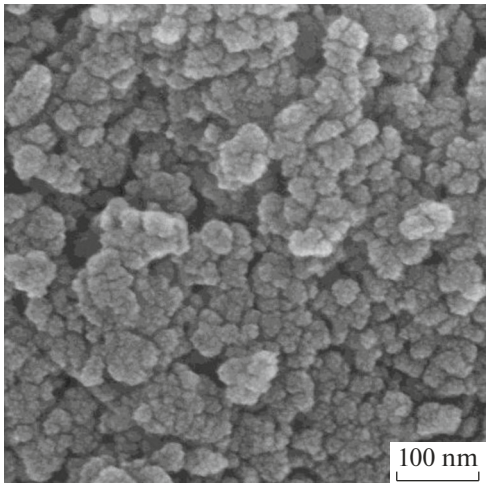

Fig. 3. Field emission scanning electron microscope image of the as synthesized hydroxyapatite nanoparticles used for the coating operation.

7.5 millimeter diameter and 30 balls with 5.5 millimeter diameter with a total weight of 120 grams. The coating process was applied for 4 h at a ball to powder ratio (BPR) of 30 : 1.

2.2.1. Synthesis of hydroxyapatite nanopowder. To perform the coating procedure on Ti–6Al–4V substrate, nanosized hydroxyapatite powder was synthesized and used. In order to prepare nanohydroxyapatite powder we extracted the fat and bone marrow of a camel femur bone and left it in an oven for 20 min at 55°C to eliminate the moisture. Then it was exposed to the flame of a torch for 160 min. The obtained bone ash was milled in a high energy planetary mill for 5 h with a ball to powder ratio of 50 : 1 and a milling speed of 300 rpm. Finally the milled ashes were exposed to thermal treatment for 90 min at 650°C as obtained by thermal analysis.

2.2.2. Coating procedure. To perform the coating operation, the synthesized nanohydroxyapatite powder along with the steel balls are placed into the vial with a ball to powder ratio of 30 : 1 and the coating process was done for 4 h. The revolution speed of the milling machine for this operation is defined to be 300 rpm.

2.3. Characterization of the Coating

In order to determine the phase purity, composition, structure and crystallite size in the coating operation X-ray diffraction (model Asenware AW-DX300) with wave length of $\lambda Cu(K_{\alpha 1})$ = 1.54184 Å was used. Furthermore the sizes of the used particles were obtained by a field emission scanning electron microscope (model Mira 3-XMU).

In the present study, quantitative phase analysis was performed by the Rietveld method using Topas4-2 software package [31]. According to the analysis pure hydroxyapatite was present.

Also for the morphology and particle size analysis of the applied hydroxyapatite nanocoating, field emission scanning electron microscopy was used. The bioactivity test, was applied on the coating by placing it in the simulated body solution (pH 7.4 and at temperature =37°C) for 14 days. Subsequently the sample was analyzed with scanning electron microscope and FTIR analysis to study on the formation of hydroxyapatite on the surface of the coating.

3. DISCUSSION

3.1. X-ray Diffraction and Rietveld Analysis of the Synthesized Nanopowders

Figure 2 shows the X-ray diffraction of the synthesized hydroxyapatite nanopowders used for the coating process.

The X-ray diffraction pattern of the used powder showed wide and broad peaks with low intensity that can be referred to the formation of nanostructured hydroxyapatite particles. The crystallite size was calculated by the Rietveld method to be 19.7 nanometers. Furthermore pure hydroxyapatite was present.

3.2. Field Scanning Electron Microscope

In Fig. 3 the field emission scanning electron microscope image for the as synthesized hydroxyapatite nanoparticles are shown.

Figure 3 confirms the presence of nanoparticles along with larger sized particles in the hydroxyapatite powder used for coating which is in an agreement with the average crystallite size obtained from the X-ray pattern by the Rietveld method. Figure 4 shows the

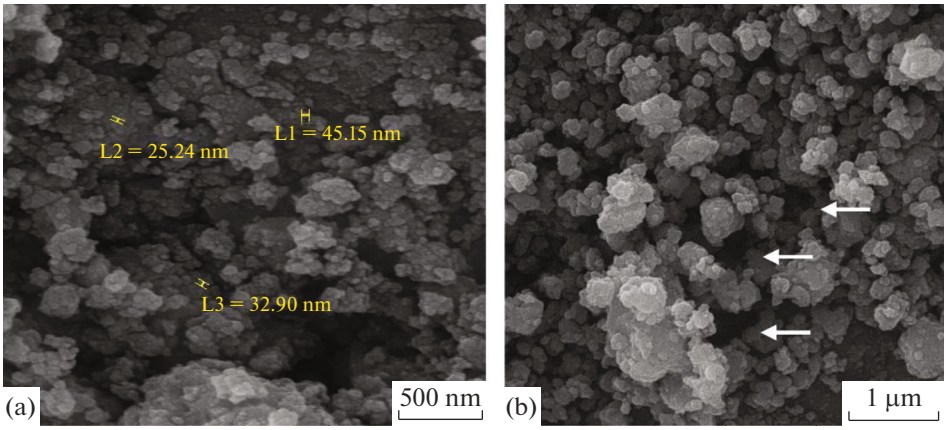

Fig. 4. Scanning electron microscopy image of the coated particles: (a) the nanometer coated particles and (b) the porosity present in the coating.

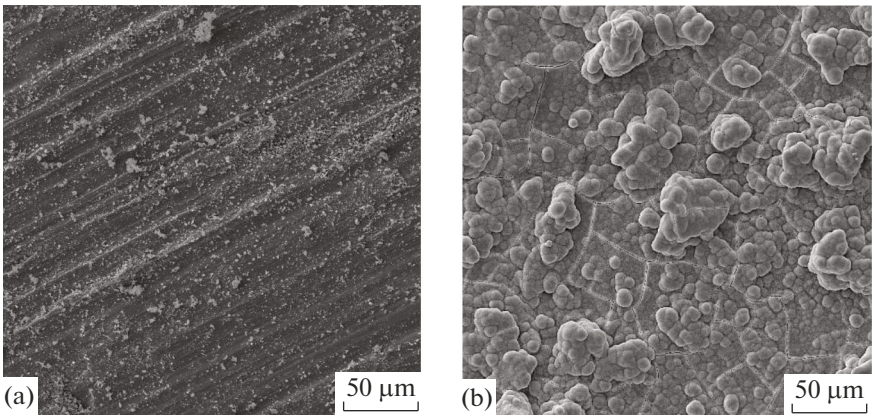

Fig. 5. Scanning Electron microscopy image of the nanohydroxyapatite coating (a) before bioactivity test and (b) after 14 days immersion in the simulated body fluid.

scanning electron microscopy image of the coated nanohydroxide particles.

Figure 4a clearly shows that the coated particles are in nanometer range. However their size is larger than the initially as synthesized nanohydroxyapatite particles. Furthermore Fig. 4b shows, the porosity present in the coating as indicated by arrows. According to Zhang et al. [32], these porosities result in the insertion of apatite inside the cavity and strengthen their binding to the coating and, therefore a significantly increased biocompatibility is possible.

3.3. Results of the Bioactivity Test

The bioactivity test on the nanohydroxyapatite coating was applied by 14 days immersion in a simulated body fluid. The sample was investigated by scanning electron microscopy before and after applying the test as shown in Fig. 5.

The comparison of Figs. 5a, 6b clearly shows the formation of hydroxyapatite on the surface of the coating showing the bioactive property of the coated sample. The coated hydroxyapatite nanoparticles have resulted in surface roughness. It has been reported that a bioactive surface with high roughness leads to the better biological stabilization of implants due to the bone growth in the pores, which is in addition to the chemical bonding as a result of physical contact.

Another point to be noted about the nanohydroxyapatite coating is that due to its high surface to volume ratio, its physical-chemical activity increases resulting in higher bioactivity which increases the rate of hydroxyapatite formation on the surface, and therefore this large amount of hydroxyapatite is formed in 14 days. Also, given that the coating itself is hydroxyapatite; therefore hydroxyapatite formation is easier and forms a stronger bond.

Also to confirm the formation of hydroxyapatite on the surface of the coating it was analyzed by Fourier transform infrared spectroscopy after the bioactivity test as shown in Fig. 6.

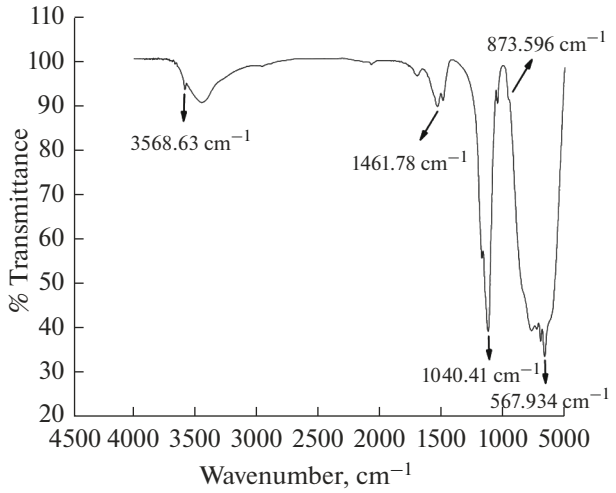

Fig. 6. FTIR analysis of the hydroxyapatite nanopowder formed on the surface of the coated substrate after the bioactivity test.

Figure 6 confirms the presence of hydroxyapatite peaks according to Chandrasekaran et al. [33], Choi et al. [34] and Cengiz et al. [35]. According to their reports it has been mentioned that the FTIR spectra of hydroxyapatite is ion stretching (OH^-) around wavenumber 3568 cm^{-1}, asymmetric stretching (CO_3^{2-}) around 1461 cm^{-1}, asymmetric stretching (PO_4^{3-}) around 1041 cm^{-1}, out of plane bending mode (CO_3^{2-}) around 869 cm^{-1} and asymmetric bending vibration (PO_4^{3-}) at around 570 cm^{-1}.

CONCLUSIONS

In this study, a milling vial was designed and introduced with the ability to simultaneously coat substrates by mechanical means. The successful coating of the as synthesized nanohydroxyapatite particles on 4V–6Al–Ti substrate was confirmed by XRD and SEM and the analysis of the results of the bioactivity test showed that the vial was able to simultaneously and uniformly coat substrates with the capability to be implanted in a living body with high bioactivity properties as confirmed by SEM and FTIR. This method can be used as a simple and economical method with the coating process having a short duration to be completed.

After the coating process the sample is easily removed from the vial without being damaged, scratched or polluted. Furthermore by optimizing the coating conditions, this method can be used to coat other types of powders or on any other substrate.

REFERENCES

1. Niespodziana, K., Jurczyk, K., Jakubowicz, J., et al., *Mater. Chem. Phys.,* 2010, vol. 123, pp. 160–165.
2. Fujisawa, A., *Kokubyo Gakkai Zasshi,* 2004, vol. 71, pp. 112–119.
3. Okazaki, Y., Rao, S., Ito, Y., Tateishi, T., et al., *Biomaterials,* 1998, vol. 19, pp. 1197–1215.
4. Song, W., Tu, B., Lin, J., et al., *Biocybern. Biomed. Eng.,* 2015, vol. 35, no. 4, pp. 296–303.
5. Webster, T.J., Ergun, C., Doremus, R.H., et al., *J. Biomed. Mater. Res., Part A,* 2003, vol. 67, pp. 975–980.
6. Bovand, D., Yousefpour, M., Rasouli, S., et al., *Mater. Des.,* 2015, vol. 65, pp. 447–453.
7. Wang, K., *Mater. Sci. Eng., A,* 1996, vol. 213, pp. 134–137.
8. Pilliar, R.M., Cameron, H.U., Welsh, R.P., et al., *Clin. Orthop. Relat. Res.,* 1981, vol. 156, pp. 249–257.
9. Tolstunov, L., *J. Oral. Implantol.,* 2014, vol. 40, pp. 365–370.
10. Chrzanowski, W., Kondyurin, A., Lee, J.H., et al., *J. Mater. Sci.: Mater. Med.,* 2012, vol. 23, pp. 2203–2215.
11. Chrzanowski, W., Szade, J., Hart, A.D., et al., *J. Biomater. Appl.,* 2012, vol. 26, pp. 707–731.
12. Jinno, T., Kirk, S.K., Morita, S., et al., *J. Arthroplasty,* 2004, vol. 19, pp. 102–109.
13. Sul, Y., Johansson, C., Byon, E., et al., *Biomaterials,* 2005, vol. 26, pp. 6720–6730.
14. Sul, Y.T., *Biomaterials,* 2003, vol. 24, pp. 3893–3907.
15. Suchanek, W. and Yoshimura, M., *J. Mater. Res.,* 1998, vol. 13, no. 1, pp. 94–117.
16. Komath, M., Varma, H.K., and Sivakumar, R., *Bull. Mater. Sci.,* 2000, vol. 23, no. 2, pp. 135–140.
17. Hench, L.L. and Kokubo, T., in *Handbook of Biomaterial Properties*, Black, J. and Hastings, G., Eds., Springer, 1998, pp. 355–363.
18. Samuneva, B., Kozhukharov, V., Trapalis, C., et al., *J. Mater. Sci.,* 1993, vol. 28, no. 9, pp. 2353–2360.
19. Hannora, A.E. and Ataya, S., *J. Alloys Compd.,* 2016, vol. 658, pp. 222–233.
20. Ratner, B.D., Hoffman, A.S., Schoen, F.J., and Lemons, J.E., *Biomaterials Science, An Introduction to Materials in Medicine,* Academic Press, 2004.

21. Wei, D., Zhou, Y., Jia, D., et al., *Ceram. Int.,* 2008, vol. 34, pp. 1139–1144.
22. Un, S. and Durucan, C., *J. Biomed. Mater. Res., Part B,* 2009, vol. 90, pp. 574–583.
23. Wang, J., Chao, Y., Wan, Q., et al., *J. Mater. Sci.: Mater. Med.,* 2009, vol. 20, pp. 1047–1055.
24. Hench, L.L. and Wilson, J., *An Introduction to Bioceramics,* vol. 1 of *Advanced Series in Ceramics,* Singapore: World Scientific Publ., 1998.
25. Fathi, M.H. and Hanifi, A., *Mater. Lett.,* 2007, vol. 61, p. 3978.
26. Fathi, M.H. and Zahrani, E.M., *J. Cryst. Growth,* 2009, vol. 311, pp. 1392–1403.
27. Xiao, X.F., Liu, R.F., and Zheng, Y.Z., *Surf. Coat. Technol.,* 2006, vol. 200, no. 14, pp. 4406–4413.
28. Bose, S., *High Temperature Coatings,* Butterworth–Heinemann, 2011.
29. Nakahira, A. and Eguchi, K., *J. Ceram. Process. Res.,* 2001, vol. 2, pp. 108–112.
30. Salman, S., Gunduz, O., Yilmaz, S., et al., *Ceram. Int.,* 2009, vol. 35, pp. 2965–2971.
31. *TOPAS. 4.1.,* Karlsruhe: Bruker AXS, 2007.
32. Zhang, B.G.X., Myers, D.E., Wallace, G.G., et al., *Int. J. Mol. Sci.,* 2014, vol. 15, no. 7, pp. 11878–11921.
33. Chandrasekar, A., Sagadevan, S., and Dakshnamoorthy, A., *Int. J. Phys. Sci.,* 2013, vol. 32, no. 8, pp. 1639–1645.
34. Choi, D., Marra, K., and Kumta, P.N., *Mater. Res. Bull.,* 2004, vol. 39, pp. 417–432.
35. Cengiz, B., Gokce, Y., Yildiz, N., et al., *Colloids Surf., A,* 2008, vol. 322, pp. 29–33.